ELSEVIER

Polymer 41 (2000) 5895–5902

polymer

Structure evolution and phase behavior of polymer blends under the influence of shear

Z. Hong[a], M.T. Shaw[a,b,*], R.A. Weiss[a,b]

[a]*Polymer Program, Institute of Materials Science, University of Connecticut, Storrs, CT 06269, USA*
[b]*Department of Chemical Engineering, University of Connecticut, 191 Auditorium Road, Room 204, U-222, Storrs, CT 06269, USA*

Received 12 March 1999; received in revised form 4 October 1999; accepted 15 October 1999

Abstract

The effect of shear flow on the phase behavior, structure formation and morphology of a near-critical composition blend of poly(styrene-*co*-acrylonitrile)/poly(methyl methacrylate) (SAN/PMMA) and an off-critical composition blend of SAN/poly(ε-caprolactone) (SAN/PCL) were investigated. Both blends exhibited lower critical solution temperature (LCST) behavior. Rheo-SALS (small angle light scattering) was used to characterize the time-dependent structure evolution during flows with shear rates from 0.01 to 0.05 s^{-1} and stresses from 8 to 60 kPa. Two types of transient "dark-streak" scattering patterns were observed. One featured a dark streak that diverged with increasing scattering vector, q, which corresponded to a chevron-like structure in the morphology of the blend. The other type of dark streak converged with increasing q, and may be due to a spinodal structure that was stretched in the flow direction. A capillary viscometer was used to achieve shear stresses as high as 400 kPa for the SAN/PCL blends, and microscopy analysis of microtomed extrudates revealed a dispersed phase morphology of cylindrical PCL-rich domains highly oriented in the flow direction. No shear-induced phase transitions were observed for either blend for the range of shear stress studied.

Keywords: Polymer blends; Stress effects; PMMA/SAN

1. Introduction

The properties of polymer blends are determined to a large extent by the morphology that is developed during the processing. As the industrial applications of polymer blends increase [1], there is an increasing need for developing a better understanding of the relationships between melt deformation history, phase behavior and morphology development. Knowledge of these relationships is necessary for understanding the origin of the morphology produced in commercial blends processes, and it also may provide the opportunity for attaining better control of the blend morphology during processing and, perhaps, achieving unique structures and properties.

Typical polymer processing procedures, e.g. extrusion or injection molding, subject the polymer blend to complicated deformations under non-isothermal conditions. The deformation field is typically heterogeneous and includes both shear and elongational strains, and it is not conducive to easy analysis, especially if one wants to know the phase behavior of a blend under stress and achieve a cause-and-effect understanding of how structure develops. Studies involving well-controlled deformations, e.g. simple shear, are much easier to accomplish, and although such deformations oversimplify an actual melt processing operation, they do provide a basis for developing an understanding of the more complicated flows.

Previous studies of the effect of flow on the phase-behavior of polymer blends have produced conclusions of both flow-induced mixing [2–16] and demixing [4,5,8,9,11–13]. These phenomenon have been ascribed to a "shift" of the phase boundary by stress. Recently, the use of more sensitive experimental techniques has brought into question some of the conclusions of the previous research. For example, one-dimensional (1D) small angle light scattering (SALS) has been used to observe phase-mixing under shear [7,10,11]. However, that technique does not consider the anisotropic nature of the deformation, and shear-induced mixing was not observed by rheo-optical studies using two-dimensional (2D) SALS measurements of similar blend systems [17–20].

In a previous paper [19], we reported on the effect of shear flow on the phase behavior and structure formation in a near critical blend of poly(styrene-*co*-acrylonitrile)/poly(methyl methacrylate) (SAN/PMMA). The system of SAN/PMMA was chosen because the glass transition

* Corresponding author. Tel.: +1-860-486-3980; fax: +1-860-486-4745.

0032-3861/00/$ - see front matter
PII: S0032-3861(99)00774-0

Table 1
Characteristics of components and blends

	Polymer	Supplier	T_g (°C)	T_m (°C)	n_D @ (20°C)	M_w (kDa)	M_w/M_n	Wt %	T_{cp} (°C) [a]
Blend 1	SAN (29 wt% AN)	Bayer Corp.	105	–	1.57	108	2.32	25	168
	PMMA	ICI Acrylics	107	–	1.49	92	1.87	75	
Blend 2	SAN (28 wt% AN)	Bayer Corp.	105	–	1.57	190	2.14	80	170
	PCL	Union Carbide	− 60	60	1.47[b]	95	1.65	20	

[a] Cloud point as determined by light scattering turbidity measurements.
[b] Estimated from group contributions.

temperatures (T_g) were similar, the blend has a convenient lower critical solution temperature (LCST) that is easily accessed in laboratory rheometers or melt processing equipment, and the T_g of the blend is sufficiently high that specimens may be quickly quenched to below T_g in order to preserve the morphology of the melt for microscopy evaluation. This paper represents a continuation of that research, and in particular it endeavors to explain some of the unusual 2D LS patterns that accompanied the shear-induced structural changes that were reported in Ref. 19. In addition, 2D rheo-SALS and microscopy studies of the high shear-rate deformation of an off-critical blend of poly(styrene-*co*-acrylonitrile) and poly(ε-caprolactone) (SAN/PCL) are also reported.

2. Experimental

2.1. Materials

Both binary blends studied, (SAN/ PMMA) and (SAN/ PCL), consisted of a random copolymer, SAN, and a homopolymer (PMMA, PCL) that are miscible only for a limited range of compositions of the copolymer [21–24]. The AN content in SAN for each blend was within the miscible range, 29 wt% AN for the blends with PMMA and 28 wt% AN for the blends with PCL. Both blends exhibit LCST-phase behavior [25]. A near-critical composition of 25/75 SAN/PMMA and an off-critical composition of 80/20 SAN/PCL were used. The high SAN content was selected to avoid complications due to the crystallization of the PCL. The characteristics of the component polymers are listed in Table 1.

The glass transition temperatures were determined using a differential scanning calorimetry (DSC). Gel permeation chromatography (GPC) was used to measure the molecular weight averages using a polystyrene calibration. GPC measurements made on the same samples before and after shear flow indicated that no polymer degradation occurred. The cloud-point temperatures (T_{cp}) for the blends were determined using a custom-built light scattering instrument [26]; specimens were prepared by solution casting the blends from 1,2-dichloroethane onto glass slides. The samples were then dried in a hood at room temperature and vacuum dried for 3 days at 100°C prior to the T_{cp} measurement.

Blends for the rheo-SALS studies were prepared by melt mixing at 150°C in a Brabender Plasticorder for 15 min with a rotor speed of 40 rpm. The blends were then compression molded into 0.8-mm-thick, 50-mm diameter disks at 150°C using a Carver hydraulic heat press. For the capillary viscometry studies, the samples were ground to small pellets using a Wiley Laboratory Mill.

2.2. Rheo-SALS measurements

Time-resolved SALS measurements on blends undergoing simple shear flow were performed with a custom-built rheo-SALS apparatus [27]. The instrument uses a Rheometrics mechanical spectrometer to control the shear flow between 50 mm diameter parallel plates. Light is provided by a 10 mW He–Ne laser. The light scattering of the melt in the plane formed by the flow and vorticity directions is projected onto a semitransparent screen, and the image is recorded with a Princeton Instruments 2D CCD camera.

The SAN/PMMA blend was heated to 180°C, which is 12°C above T_{cp}, between the parallel plates of the rheo-SALS instrument until the sample was well phase-separated. Shear was then applied, and the time-resolved 2D light scattering patterns were recorded. The experimental procedure for the SAN/PCL blend was similar, except that 180°C was ~10°C above T_{cp}. Shear experiments for the SAN/PCL blend were also carried out at 165°C, which is 5°C below T_{cp}, to evaluate if flow perturbed the structure of the miscible blend melt.

2.3. Capillary viscometry and transmission electron microscopy

Higher shear-rate melt flows were achieved with an Instron MCR Capillary Viscometer using capillaries with aspect ratios (L/D) of 20 and 40 and diameters of 2.54 and 1.27 mm, respectively. The extrudate from the Instron capillary viscometer was quenched in a dry-ice slush within one-quarter-inch of the die exit, and the strand was then microtomed in both the flow and transverse directions for microscopy studies. The specimens were cut at a radial position approximately three-fourths of the strand radius, measured from the center of the sample, to avoid edge effects. A

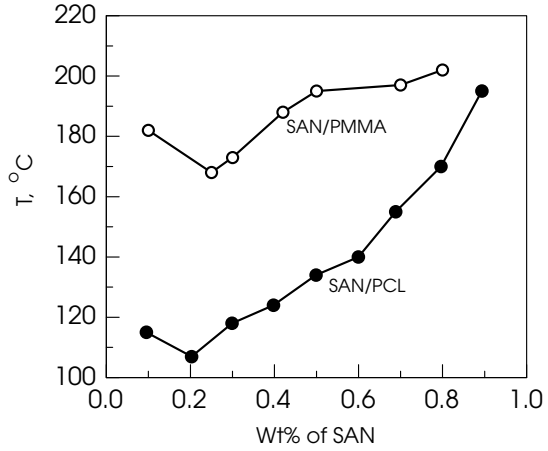

Fig. 1. Cloud point curves for SAN/PMMA and SAN/PCL blends. Heating rate = 1°C/min.

Philips-300 transmission electron microscope (TEM) was used to image the microtomed specimens. Ruthenium tetraoxide vapor was used to stain the SAN/PCL samples, which produced light SAN-rich domains and dark PCL-rich domains in the micrographs.

3. Results and discussion

3.1. Phase diagrams

The phase diagrams of the two blends are shown in Fig. 1. For the SAN/PMMA system, the critical composition is between 15 and 25 wt% SAN, and a near-critical composition, 25/75 SAN/PMMA, with $T_{cp} = 168°C$ was chosen for this study. For the SAN/PCL system, an off-critical composition of 80/20 SAN/PCL with a $T_{cp} = 170°C$ was used.

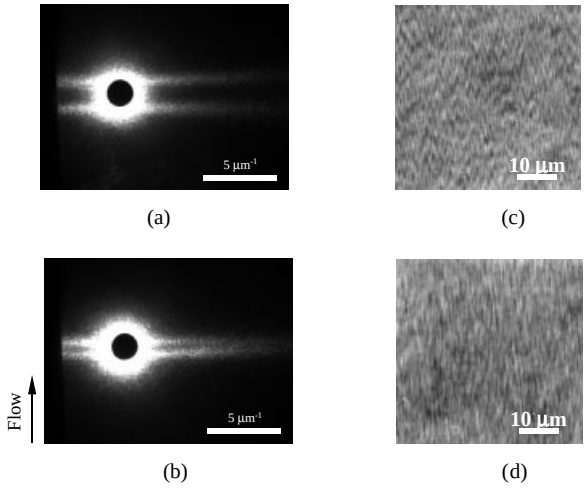

Fig. 2. Time-resolved 2D light scattering patterns of a phase-separated 25/75 SAN/PMMA blend subjected to a shear rate of 0.02 s^{-1}, and the corresponding microstructures of the quenched sample: (a) divergent pattern, $\gamma = 7.9$; (b) convergent pattern, $\gamma = 73.8$; (c) chevron structure; (d) deformed spinodal structure.

3.2. Rheo-SALS of near-critical SAN/PMMA blend

In our previous paper [19], we showed that when a near-critical SAN/PMMA blend below its T_{cp} was subjected to shear stresses less than 60 kPa, the SALS patterns evolved from a classical spinodal-ring to a pattern characterized by two light lobes or "wings" separated by a "dark-streak", and eventually to a "bright-streak" pattern. Microscopy observations of samples that were fast-quenched at various stages of the polymer deformation (i.e. as a function of shear strain) revealed that the phase structure evolved from a bicontinuous spinodal structure, to a chevron-like structure, and finally to a steady-state fibrillar structure.

New results reported in the present paper provide some insight into the origin of the morphology evolution that was reported in Ref. [19]. Time-resolved rheo-SALS experiments revealed two types of dark-streak scattering patterns: (1) a "butterfly" shaped pattern with two wings (or the locus of maximum intensity) that diverged at the tip (see Fig. 2(a)), and (2) an "H-shaped" pattern where the two wings converged at the tip (see Fig. 2(b)). In all the scattering images shown in this paper, the central black spot is due to the beam stop, and the gray scale represents the intensities of scattered light—the brighter the image, the higher the light intensity. The two scattering patterns shown in Fig. 2(a) and (b) correspond to two distinctly different phase structures. Phase-contrast optical micrographs of the sample morphologies that corresponded to Fig. 2(a) and (b) were obtained from samples that were quenched to below room temperature to preserve the morphology developed during flow. The diverging SALS pattern corresponds to a chevron-like structure in real-space (see Fig. 2(c)) and the converging pattern arises from the structure shown in Fig. 2(d), which we call a "deformed spinodal" structure. The deformed spinodal structure was previously reported for polybutadiene/polyisoprene blends and was shown to develop from a spinodal structure by growth of the concentration periodicity in the flow direction during shear deformation, while the periodicity of the concentration heterogeneity in the vorticity direction remained unchanged [18]. To distinguish between the two patterns shown in Fig. 2, we will refer to them as either "divergent" or "convergent".

Figs. 3–6 show the effect of shear flow on the SALS of the SAN/PMMA blend for a shear rate of 0.02 s^{-1}. For low shear strains, γ, a divergent scattering pattern was observed. A three-dimensional (3D) surface plot of the pattern is shown in Fig. 3(a), where height represents relative intensity. Note that the incident light beam was not centered on the detector, so that the scattering patterns shown in this paper are not symmetrical in that the two left quadrants of the scattering pattern were truncated at a lower value of the scattering vector, q ($q = 4\pi \sin\theta/\lambda$, λ is the wavelength of the light and 2 θ is the scattering angle). Fig. 3(a) shows that the two ridges of intensity diverge at high scattering vectors. Slices of the I vs. $q_{\|}$ (the scatter vector parallel to the flow

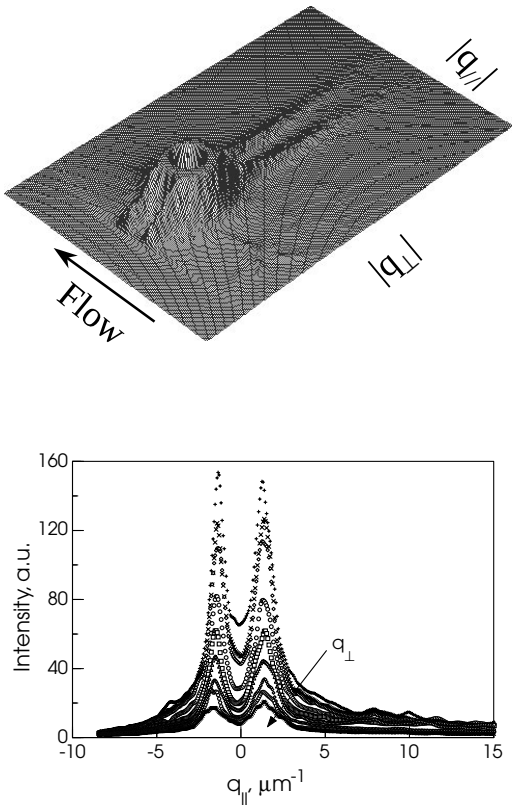

Fig. 3. Characteristics of the divergent scattering pattern (shear rate = $0.02\ s^{-1}$) at $\gamma = 7.9$: (a) 3D surface plot, where height is the relative scattering intensity; (b) 2D plot of intensity distributions of different $q_\perp$ in the directions parallel ($q_\parallel$) to the flow. (Curves are shifted vertically for visual clarity.)

direction) plane made at different values of $q_\perp$ (the scattering vector parallel to the vorticity direction) are plotted in Fig. 3(b); the curves are shifted vertically for clarity. The maximum intensity decreases with increasing $|q_\perp|$, and the separation of the two intensity maxima increases. The separation of the two peaks, $|\Delta q_{\parallel\max}|$ is plotted against

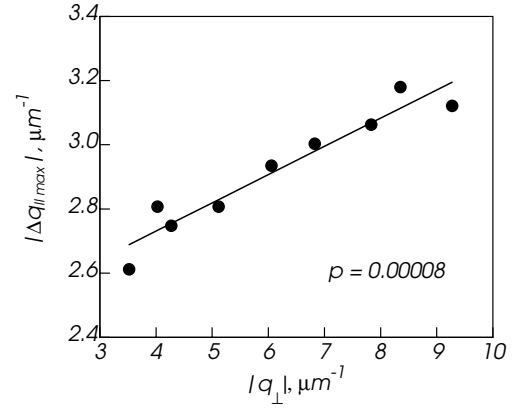

Fig. 4. Characteristics of the divergent scattering pattern (shear rate = $0.02\ s^{-1}$) at $\gamma = 7.9$: distance between two intensity peaks ($|\Delta q_{\parallel\max}|$) relative to the scattering vector magnitude perpendicular to the flow ($|q_\perp|$).

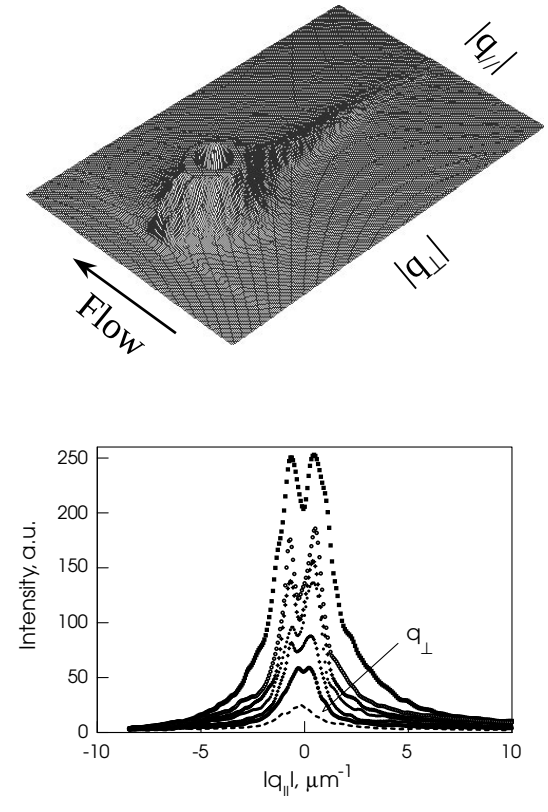

Fig. 5. Characteristics of the convergent scattering pattern (shear rate = $0.02\ s^{-1}$) at $\gamma = 73.8$: (a) 3D surface plot, where height is the relative scattering intensity; (b) 2D plot of intensity distributions of different $q_\perp$ in the directions parallel ($q_\parallel$) to the flow. (Curves are shifted vertically for visual clarity.)

$|q_\perp|$ in Fig. 4. Here, p, which is determined by statistical analysis of the data, is the probability of error by rejecting the hypothesis that $|\Delta q_{\parallel\max}|$ does not increase with $|q_\perp|$. The small value of $p = 0.00008$ confirms that the scattering pattern is indeed divergent. A puzzling, and as yet unexplained, result is that the intercept of the plot at $|q_\perp| = 0$ is $|\Delta q_{\parallel\max}| = 2.38 \pm 0.15\ \mu m^{-1}$, rather than zero, which is the expected intercept for a pattern corresponding to a chevron structure.

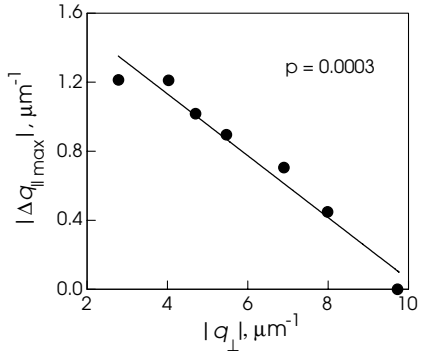

Fig. 6. Characteristics of the convergent scattering pattern at $\gamma = 73.8$: distance between two intensity peaks ($|\Delta q_{\parallel\max}|$) relative to the scattering vector magnitude perpendicular to the flow ($|q_\perp|$).

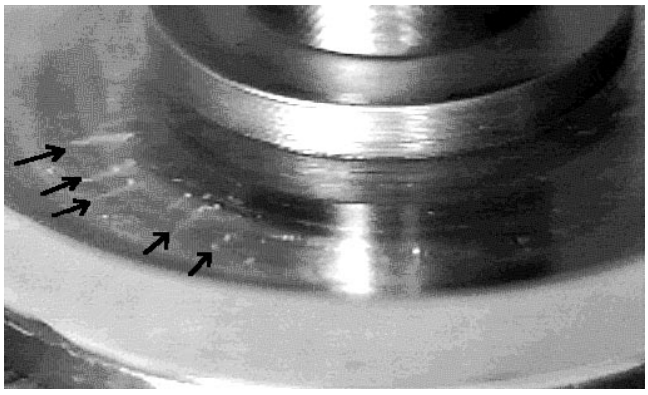

Fig. 7. Flow instability of an 80/20 SAN/PCL blend at a shear rate of 1 s^{-1} in parallel-plates.

In contrast to the scattering patterns shown in Fig. 3, at higher shear strain the SALS pattern was convergent. The 3D surface plot in Fig. 5(a) shows that the ridges corresponding to the maximum intensities merge at high q; this is clearly seen in the I vs. $q_{\parallel}$ in Fig. 5(b). Fig. 6 shows that $|\Delta q_{\parallel \max}|$ decreases with increasing $|q_{\perp}|$, and, again, the small probability ($p = 0.0003$) supports the conclusion that the scattering pattern converges.

3.3. Formation of the chevron-like structure

The observations reported here and in a previous paper [19] suggest that the chevron-like structure shown in Fig. 2(c), which is associated with the divergent SALS pattern, is an intermediate morphology that arises when stress is first applied to a near-critical blend. The origin of this unusual morphology is still open to speculation. Remediakis et al. [20] proposed that secondary flows similar to the helical flows in the vorticity direction reported by Kulicke et al. [28,29] may be responsible for the chevron-like morphology. For highly elastic melts, parallel torsional flow can produce a secondary flow with a velocity component in the vorticity direction. Superposition of the primary and secondary flows produces a velocity vector at an angle out of the θ–z plane (i.e. the plane formed by the flow and shear gradient directions) that results in a helical flow propagating radially outward from the plates. For a two-phase melt, one might expect that the dispersed phase being stretched by the primary flow field will assume orientations tangential to a helix. The projection on the θ–r plane (i.e. the plane formed by the flow and vorticity directions, which is what the SALS probes) will appear as anisotropic domains oriented at an angle or angles to the flow direction. This could conceivably give the appearance of a zigzag or chevron-like pattern, while in reality the structure is 3D. In addition, the absence of any domains oriented parallel to the flow direction reduces scattering along the equator of the SALS pattern, which will produce a dark streak.

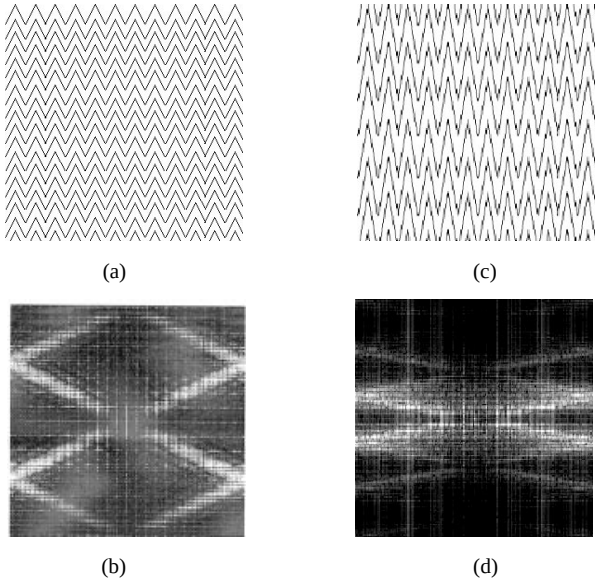

Fig. 8. Simulated zigzag shape of a tilted domain structure and its FT: (a) zigzag; (b) FT of (a); (c) deformed zigzag; (d) FT of (c).

Observations made in this study of irregular distortions in the flowing SAN/PMMA (and SAN/PCL) melts at moderate shear rates appears to support that hypothesis. Fig.7 shows a series of azimuthally spaced vortices propagating in the vorticity direction that were observed for the 80/20 SAN/PCL blend at a shear rate of 1 s^{-1}. Although the connection between the flow instability observed in Fig. 7, the SALS pattern and the chevron-like structure shown in Fig. 2(a) and (c) is speculative, it does establish a working hypothesis for further investigations.

Fig. 8 shows two zigzag representations of tilted domain structures and their Fourier transforms (FT); Fig. 8(a) was stretched to produce Fig. 8(c). The similarity between the FT patterns and the divergent SALS pattern shown in Fig. 2(c) is apparent. Both possess a dark streak, which presumably arises from the suppression of domains aligned in the flow direction. Because the orientation of the polymer domains is probably not as regular as the ideal zigzag structures drawn in Fig. 8, the SALS pattern in Fig. 2(c) is not as well-defined as the FTs in Fig. 8 (b) and (c). In addition, multiple scattering may tend to smear the features the SALS patterns produced by the polymer sample. Nonetheless, it

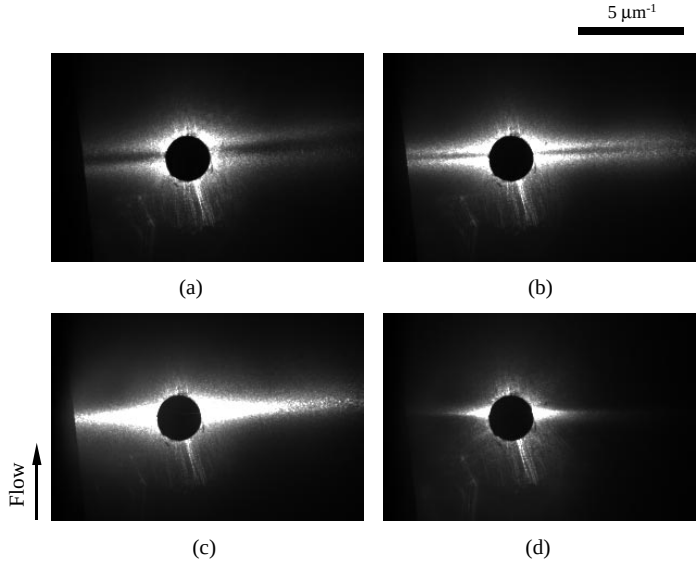

Fig. 9. Time-resolved light scattering patterns for 80/20 SAN/PCL at 180°C (a)–(c): shear rate = 0.1 s^{-1}, shear stress = 7.6 kPa; (a) $\gamma = 54$; (b) $\gamma = 72$; (c) $\gamma = 186$; (d) shear rate = 1 s^{-1}, shear stress = 44 kPa, $\gamma = 732$.

appears reasonable to hypothesize that the chevron-like morphology is responsible for the divergent scattering pattern. However, as mentioned above, extrapolation of the intensity maxima of the diverging wings on each side of the dark streak gives a positive intercept at zero scattering angle, a result that is inconsistent with that expected for scattering from a zigzag structure.

3.4. Rheo-SALS of off-critical SAN/PCL blend

The off-critical composition, 80/20 SAN/PCL, blend was well phase-separated after annealing at 180°C and appeared cloudy. When it was sheared, however, the appearance of the sample gradually changed from cloudy to clear, though the SALS patterns indicated that the blend was still phase separated. A video of the time-resolved SALS patterns at 180°C (i.e. 10°C above T_{cp}) and a shear rate of 0.01 s^{-1} (shear stress, $\tau = 487$ Pa) is available in a file named san_p-cl.avi [30]. Upon the application of shear flow, the SALS evolved from an isotropic pattern for a dispersed spherical phase to a divergent butterfly pattern. With increasing γ the separation of the wings of the divergent pattern decreased (i.e. the dark streak became narrower), and eventually the pattern evolved into a bright streak along the equator of the scattering pattern. This behavior, which is for an off-critical composition, was similar to that which was previously observed for the near-critical blend of SAN/PMMA [19].

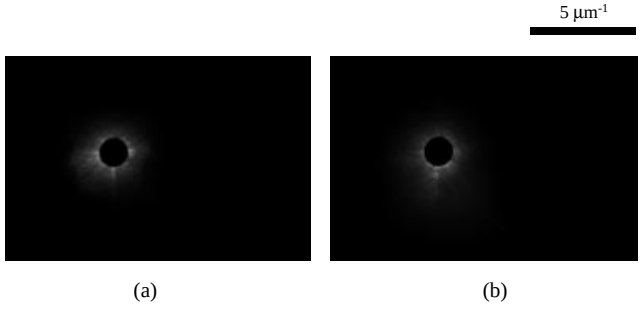

Fig. 10. Time-resolved light scattering patterns of 80/20 SAN/PCL at 160°C under a shear rate of 0.05 s^{-1}, shear stress of 12.2 kPa: (a) $\gamma = 0$; (b) $\gamma = 315$.

Fig. 9 shows time-resolved scattering patterns for the SAN/PCL blend undergoing shear flow at 180°C and a shear rate of 0.1 s^{-1}. The unsheared sample exhibited a spinodal ring. Shearing the sample produced the divergent pattern shown in Fig. 9(a). As the strain increased, the separation between the two wings of the scattering pattern became narrower, see Fig. 9(b) and eventually disappeared, and a bright streak pattern that did not change with time eventually formed (see Fig. 9(c)). The bright streak pattern corresponds to a blend morphology consisting of fibrillar domains oriented in the flow direction. When the shear rate was increased a decade higher to 1 s^{-1}, the bright streak immediately shortened, Fig. 9(d), which indicates further elongation of the domains. The steady-state scattering pattern was the bright streak, even though the sample was optically clear. Higher shear rates were not possible to achieve with the rheo-SALS instrument without introducing flow instabilities.

A sample of the 80/20 SAN/PCL blend was also annealed at 160°C, which is 10°C below T_{cp}, for 1 h and then subjected to a steady shear rate of 0.05 s^{-1} ($\tau = 12.2$ kPa). SALS patterns of the sample before and during shearing are shown in Fig. 10. The unsheared blend ($\gamma = 0$) was miscible and the resulting scattering pattern was isotropic. In Fig. 10, the bright regions adjacent to the beam stop were due to reflections off the beam stop and the instrument optics. The scattering pattern was unaffected by shearing, even

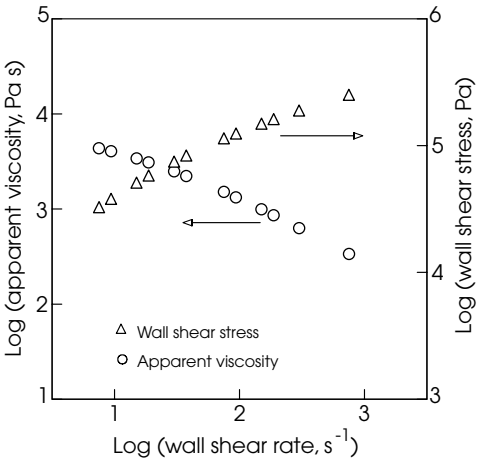

Fig. 11. Flow properties of the SAN/PCL blend at 180°C.

after the sample was sheared for 2 h. That result indicates that no large-scale concentration fluctuations developed. Flow instabilities, however, were observed when higher shear rates or shear stresses were applied. No evidence of shear-induced demixing, as has been reported for other blends [4,5,10,17], was found.

Higher shear rate flows were achieved for the 80/20 SAN/PCL by using a capillary viscometer. The flow curve at 180°C is shown in Fig. 11. No discontinuities were observed as might arise if the melt underwent a phase transition. The SAN/PCL blend had a lower viscosity than the SAN/PMMA blend and a much shorter relaxation time. The extrudate from the capillary was quickly quenched in dry-ice slush and then microtomed for TEM evaluation. TEM images of the blend extruded at a shear rate of 37.5 s^{-1} and a wall shear stress of 95 kPa are shown in Fig. 12. The TEM pictures of the r–θ and the z–r planes (Fig. 12(a) and (b) respectively) are consistent with a morphology of cylindrical PCL-rich domains dispersed in the SAN-rich matrix and highly oriented in the flow (z) direction. This is not surprising, in that phase separation of an off-critical composition is expected to produce dispersed droplets of the minor component, and strong shear stresses should elongate and align the droplets in the flow direction. No stress-induced phase transitions were observed for shear rates as high as 37.5 s^{-1} and shear stresses as high as 95 kPa.

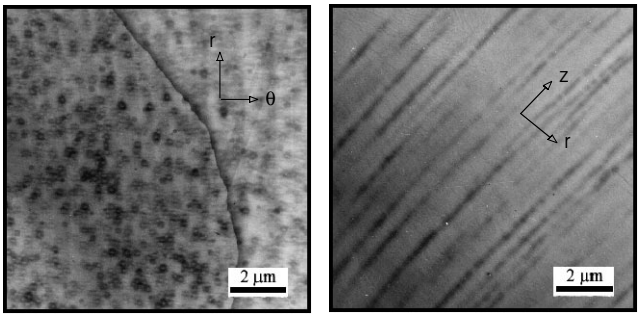

(a) (b)

Fig. 12. TEM images of a quenched SAN/PCL sample after being sheared at 180°C under a shear rate of 37.5 s^{-1} with wall shear stress of 95 kPa: (a) r, θ plane; (b) r, z plane (z is the flow direction).

Retention of the morphology in the extrudate for microscopy analysis was possible, because quenching of the specimen to ~−70 °C was quick enough so that the cylindrical rods formed during the extrusion did not have sufficient time to retract or break up. When the SAN/PCL extrudate was slowly cooled in air, the blend became completely transparent due to remixing of the components and the TEM images were homogeneous and featureless. This result indicates that for LCST-type binary blends, the quenching rate is the key for preserving the microstructure. If the temperature is lowered too slowly, the blend, especially one with a relatively low viscosity like the SAN/PCL system, may have sufficient time to equilibrate into a single phase.

4. Conclusion

The effect of simple shear flow on the morphology and phase behavior of a near-critical blend, SAN/PMMA, and an off-critical blend, SAN/PCL, were studied. When shear was applied to a phase-separated blend, the structure of the phase domains evolved from bicontinuous to chevron-like, and finally to fibrillar. Two types of dark-streak scattering patterns, divergent and convergent, were observed. The divergent pattern was associated with a chevron-like two-phase morphology, and the convergent pattern was due to an elongated spinodal-like structure. The former morphology was observed at lower shear strains, and it evolved into the latter as the strain increased. Time-resolved light scattering measurements and the microscopy studies for both blends showed no evidence of shear-induced phase transitions.

Acknowledgements

This work was supported by the Polymer Compatibilization Research Consortium at the University of Connecticut. We thank Dr M. Cantino and Ms L. Khairallah for the TEM analyses, and Dr A. Padwa for supplying SAN.

References

[1] Utracki LA. Polymer alloys and blends: thermodynamics and rheology, New York: Oxford University Press, 1989.
[2] Mazich KA, Carr SH. J Appl Phys 1983;54:5511.
[3] Rector CM, Mazich KA, Carr SH. J Macromol Sci, Phys 1988;B27:421.
[4] Katsaros JD, Malone MF, Winter HH. Polym Bull 1986;16:83.
[5] Katsaros JD, Malone MF, Winter HH. Polym Eng Sci 1989;29:1434.
[6] Lyngaae-Jorgenson J, Sondergaard K. Polym Eng Sci 1987;27:351.
[7] Kammer HW, Kummerloewe C, Kressler J, Meliot JP. Polymer 1991;32:1488.

[8] Mani S, Malone MF, Winter HH, Halary JL, Monnerie L. Macromolecules 1991;24:5451.
[9] Mani S, Malone MF, Winter HH. Macromolecules 1992;25:5671.
[10] Hindawi I, Higgins JS, Galambos AF, Weiss RA. Macromolecules 1990;23:670.
[11] Hindawi IA, Higgins JS, Weiss RA. Polymer 1992;33:2522.
[12] Fernandez ML, Higgins JS. ACS Polym Mater Sci Eng 1994;71:39.
[13] Chopra D, Vlassopoulos D, Hatzikiriakos SG. J Rheol 1998;42:1227.
[14] Nakatani AI, Kim H, Takahashi Y, Matsushita Y, Takano A, Bauer BJ, Han CC. J Chem Phys 1990;93:795.
[15] Fernandez ML, Higgins JS, Horst R, Wolf BA. Polymer 1995;36:149.
[16] Fernandez ML, Higgins JS, Richardson SM. Polymer 1995;36:931.
[17] Chen ZJ, Wu R-J, Shaw MT, Weiss RA, Fernandez ML, Higgins JS. Polym Eng Sci 1995;35:92.
[18] Chen ZJ, Shaw MT, Weiss RA. Macromolecules 1995;28:648.
[19] Hong Z, Shaw MT, Weiss RA. Macromolecules 1998;31:6211.
[20] Remediakis NG, Weiss RA, Shaw MT. Rubber Chem Technol 1997;70:71.
[21] Fowler ME, Barlow JW, Paul DR. Polymer 1987;28:1177.
[22] Suess M, Kressler J, Kammer HW. Polymer 1987;28:957.
[23] Chiu SC, Smith TG. J Appl Polym Sci 1984;29:1797.
[24] Jo WH, Chae SH, Lee MS. Polym Bull 1992;29:113.
[25] McMaster LP. Adv Chem Ser 1975;142:43.
[26] Moonay DJ, Wu RJ, Shaw MT. Proc Soc Plastics Eng, ANTEC 1994;40:2038.
[27] Wu R, Shaw MT, Weiss RA. Polym Mater Sci Eng 1993;68:264.
[28] Kulicke WM, Jeberien HE, Kiss G, Porter RS. Rheol Acta 1979;18:711.
[29] Kulicke WM, Porter RS. J Appl Polym Sci 1979;23:953.
[30] See Polymer web site: address for video.